

Eyring Powellnanofluid flow over a rotating disk with Activation energy and thermal radiation

CH. Narasimha Raju¹, V. Dharmaiah²

¹Assistant professor, Department of Mathematics, Government Degree College, Ramannapet, Yadadri-Bhongir (Dist.), Telangana, India

Email Id: chennojunarasimharaju@gmail.com

²Professor, Department of Mathematics, Osmania University, Hyderabad, Telangana, India

Email Id: vdhmathsou@gmail.com

Abstract

This paper's goal is to investigate the Eyring-Powell nano liquid past rotating disk. Thermal radiation and chemical reaction have been used to study heat and mass transmission. Convective characteristics, as well as heat and mass conditions, are studied. Through appropriate transformations, highly non-linear partial differential equation systems are transformed into non-linear ordinary differential equations. Implementing bvp4c uses the transmuted ordinary differential equations. Through graphical representation, the effects of promising physical characteristics have been investigated.

Keywords: Rotating disk, Thermal radiation, Activation energy, Eyring-Powell.

1. Introduction

Realistic and essential significant of the flows in the engineering and industry applications are encountered through non-Newtonian fluid. Such non-Newtonian applications are molten plastic, paints, food, shampoos and many more. So, the non-Newtonian fluid contributes the important part to develop the mathematical flow modeling [19,1,6]. There is no single constitutive model of non-Newtonian fluids which envisage all sorts of fluid. Few attempts are prepared to study of establishment of meaningful relationship amid the kinds of non-Newtonian fluids. To overcome these challenge, one of the most simple and ease model namely Eyring-Powell fluid model [16] was introduced by Eyring and Powell in 1944. Moreover, this model has certain benefit over other non-Newtonian fluid models. Eyring-Powell model obtained kinetic theory of gases instead of experimental relation. Khan et al. [11] described 3D flow of Eyring-Powell fluid with slip effect and heat travel past a rotating disk. Ibrahim [7] have examined the 3D flow of Eyring-Powell nanofluid over a rotating disk with heat transferring models. Recently, Gholina et al. [4] explored the Eyring-Powell rotating disk and MHD flow with physical effect. C.Srinivas Reddy et al [25] examined MHD boundary layer flow with heat and mass transfer of Casson nanofluid across a non-linear stretching sheet with viscous dissipation and radiation effect. MHD free convective heat and mass transfer from a vertical surface embedded in a non-Darcy porous medium with two stratifications was investigated by Kishan.N et al [26]. The effect of magneto hydrodynamic boundary layer flow and heat transfer of nanofluid over a permeable shrinking sheet with wall mass suction and heat source sink is described in the paper of C.Srinivas Reddy et al [27].

In a modern era, it has been anticipated to assorted nanoparticles with range $< 100nm$ and base fluid contains oil, water, ethylene glycol to form the fluid known as nanofluid. A significant heat transfer phenomenon of nanofluid is more prominent than that of base fluid have favorable in

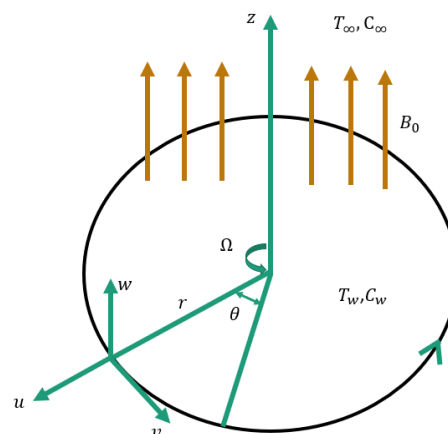
many industrial and engineering process. An application of nanofluid contains heat exchange, treatment of cancer and thermal engineering. The term nanofluid coined by Choi [22]. Buongiorno [8] evaluated the characteristics of nanofluid through the Brownian and thermophoretic diffusion. The heat transport past a rotating disk is explored by Bachok et al. [2]. Rashidi et al. [21] conducted the MHD flow of entropy generation due to a rotating porous disk in a nanofluid. The flow and heat transfer mechanism past a rotating disk has been studied by Turkyilmazoglu [23]. Ramzan et al. [20] numerically proposed the MHD flow of nanofluid past a rotating disk with slip effect. Additional inquiry on nanofluid has been explored ref. [24,10,12].

Fluid flow on Rotating disk plays a remarkable part in various industries like thermal engineering, electronic gadget and many more. So, lot of studies [17,5,13] has been done by researchers regarding this field. MHD flow of Williamson fluid on rotating disk in the influence of dissipative flow is carried out by Qayyum et al. [18]. Jyothi et al. [9] evaluated the MHD flow of CNTs nanofluid past a rotating stretched disk with thermal radiation. Pourmehran et al. [15] performed the thermal analysis of nanofluid due to rotating disk using of Brownian movement. The study of MHD flow Power law nanofluid between infinite rotating disk expanded by EL-Dabe NT et al. [3].

This article is committed to examine the chemical reaction on Eyring-Powell nanofluid due to rotating disk with activation energy. The PDE's are rendered into highly non-linearly ODE. Further, the influence of various physical emerging parameters on velocity, temperature and concentration of nanoparticles, heat transfer rate has been noted and examined through graphical representation.

2. Problem Formulation

The present articles deal the Eyring-Powell nanofluid due to a rotating disk with activation energy and chemical reaction. The mathematical model of the disk is assisted with coordinates (r, φ, z) and Ω represents the rotation rate of disk. It is assumed that T_w, T_∞ represent temperature at the surface of rotation of disk and ambient fluid temperature. The nanoparticle of volume fraction of ambient fluid is denoted by C_∞ . The graphic below depicts the flow configuration and coordinate system.



Physical Diagram of the problem

The boundary layer approximation of the governing flow problem is

$$\frac{\partial u}{\partial r} + \frac{u}{r} + \frac{\partial w}{\partial z} = 0 \tag{1}$$

$$u \frac{\partial u}{\partial r} - \frac{v^2}{r} + w \frac{\partial u}{\partial z} = v \frac{\partial^2 u}{\partial z^2} + \frac{1}{\rho\beta c} \frac{\partial^2 u}{\partial z^2} - \frac{1}{\rho\beta c^3} \left(3 \left(\frac{\partial u}{\partial z} \right)^2 \frac{\partial^2 u}{\partial z^2} + \left(\frac{\partial v}{\partial z} \right)^2 \frac{\partial^2 u}{\partial z^2} \right) - \frac{\sigma B_0^2}{\rho} u \tag{2}$$

$$u \frac{\partial v}{\partial r} + \frac{uv}{r} + w \frac{\partial v}{\partial z} = v \frac{\partial^2 v}{\partial z^2} + \frac{1}{\rho\beta c} \frac{\partial^2 v}{\partial z^2} - \frac{1}{\rho\beta c^3} \left(3 \left(\frac{\partial v}{\partial z} \right)^2 \frac{\partial^2 v}{\partial z^2} + \left(\frac{\partial u}{\partial z} \right)^2 \frac{\partial^2 v}{\partial z^2} \right) - \frac{\sigma B_0^2}{\rho} v \tag{3}$$

$$u \frac{\partial T}{\partial r} + w \frac{\partial T}{\partial z} = \alpha \frac{\partial^2 T}{\partial z^2} + \tau \left[D_B \frac{\partial C}{\partial z} \frac{\partial T}{\partial z} + \frac{D_T}{T_\infty} \left(\frac{\partial T}{\partial z} \right)^2 \right] - \frac{1}{\rho c_p} \frac{\partial q_r}{\partial z} \tag{4}$$

$$u \frac{\partial C}{\partial r} + w \frac{\partial C}{\partial z} = D_B \frac{\partial^2 C}{\partial z^2} + \frac{D_T}{T_\infty} \frac{\partial^2 T}{\partial z^2} - K_r^2 \left(\frac{T}{T_\infty} \right)^n \exp \left(\frac{E_a}{\kappa T} \right) (C - C_\infty) \tag{5}$$

Boundary conditions for the above problem are

$$u = ar, v = \Omega r, w = 0, -k \frac{\partial T}{\partial z} = h(T_w - T), D_B \frac{\partial C}{\partial z} + \frac{D_T}{T_\infty} \frac{\partial T}{\partial z} = 0 \text{ at } z = 0$$

$$u = 0, v = 0, w = 0, T = T_\infty, C = C_\infty \text{ at } z \rightarrow \infty \tag{6}$$

Introducing the following similarity transformations

$$\eta = \sqrt{\frac{\Omega}{\nu}} z, u = r\Omega F, v = r\Omega G, w = \sqrt{\Omega \nu} H, \theta(\eta) = \frac{T - T_\infty}{T_w - T_\infty}, \phi(\eta) = \frac{C - C_\infty}{C_\infty} \tag{7}$$

By using above similarity transformations equations (1)-(7) reduces to

$$H' + 2F = 0 \tag{8}$$

$$(1 + K_1)F'' - K_1 K_2 Re(3F'^2 F'' + G'^2 F'' + 2F'G'G'') - F^2 + G^2 - HF' - MF = 0 \tag{9}$$

$$(1 + K_1)G'' - K_1 K_2 Re(3G'^2 G'' + F'^2 G'' + 2F'G'F'') - 2FG - HG' - MG = 0 \tag{10}$$

$$\theta''(1 + Rd) - Pr H \theta' + Pr(Nb\theta'\phi' + Nt\theta'^2) = 0 \tag{11}$$

$$\phi'' - ScH\phi' + \frac{Nt}{Nb}\theta'' - Sc Ch(1 + \delta\theta)^n \exp\left(\frac{-E}{1 + \delta\theta}\right)\phi = 0 \tag{12}$$

The associate boundary conditions are

$$F(0) = s, G(0) = 1, H(0) = 0, \theta'(0) = -Bi(1 - \theta(0)), Nb\phi'(0) + Nt\theta'(0) = 0$$

$$F \rightarrow 0, G \rightarrow 0, \theta \rightarrow 0, \phi \rightarrow 0 \text{ as } \eta \rightarrow \infty. \tag{13}$$

Where $(K_1 = \frac{1}{\mu\rho c})$ and $(K_2 = \frac{\Omega^2}{c^2})$ are fluid parameter, $(Re = \frac{\Omega r^2}{\nu})$ is Reynolds number, $(Ma = \frac{\sigma B_0^2}{\rho\Omega})$ is Hartmann number, $(Pr = \frac{\nu}{\alpha})$ is Prandtl number, $(Nt = \frac{\tau D_T (T_w - T_\infty)}{T_w})$ is Brownian motion parameter, $(Nb = \frac{\tau D_B C_\infty}{\nu})$ is thermophoresis parameter, $(Sc = \frac{\nu}{D_B})$ is Schmidt number, $(\delta = \frac{(T_w - T_\infty)}{T_\infty})$ is temperature difference, $(E = \frac{E_a}{T_\infty k_1})$ is activation energy $(Rd = \frac{16\sigma * T_\infty^3}{3kk*})$ is radiation parameter, $(Ch = \frac{K_r^2}{\Omega})$ is chemical reaction parameter and $(s = \frac{a}{\Omega})$ is the slip parameter.

The physical quantity of interest Nu_r is defined as

$$Nu_r = \frac{r q_w}{k(T_w - T_\infty)} \tag{14}$$

$$\text{Where } q_w = - \left(\frac{16\sigma * T_\infty^3}{3k*} + k \right) \frac{\partial T}{\partial z} \Big|_{z=0} \tag{15}$$

And dimensionless expression is

$$Re^{-1/2} Nu_r = -(1 + Rd)\theta'(0), \tag{16}$$

Where $Re^{1/2} = r \sqrt{\frac{\Omega}{\nu}}$ is Reynoldsnumber.

3. Results and Discussions

The numerous physical emerging parameters on the flow field, temperature and concentration fields has been portrayed in Fig. 1-11. Table 1 displays that the existence of $F'(0)$, $-G(0)$, $-\theta(0)$ with previous literature through [14] which shows an excellent agreement. The behaviors of velocity slip parameters (s) on the different fields of $F(\eta)$, $G(\eta)$, $H(\eta)$, $\theta(\eta)$ and $\phi(\eta)$ are presented in Figs. 1-2. It is clear from Fig. 1 the velocity field and associated thermal boundary layer thickness enhances for larger value of (s). Figs. 1-2 shows that the slowly decline in $G(\eta)$, $H(\eta)$, $\theta(\eta)$ and $\phi(\eta)$ for numerous value of (s). The influence of magnetic parameters on the $F(\eta)$, $G(\eta)$, and $H(\eta)$ are prescribed in Fig. 3. It is evaluated that as magnetic field increases with depreciated the velocity field. Physically, imposition of the vertical magnetic force owing to this electrically producing fluid generates a drag force known as Lorentz force. This force has tendency to steady the flow near the disk. This shown by reducing in $F(\eta)$, $G(\eta)$, and $H(\eta)$ as (Ma) enhances.

The influences of fluid parameter (K_1) on the $F(\eta)$, $G(\eta)$, and $H(\eta)$ profiles are illustrated in Fig. 4. From this figure profiles of $F(\eta)$, $G(\eta)$, enhances with an enhanced in (K_1). It is the matter of the fact that the velocity of fluid reduces with the steady enhances in (K_1). Thus both profiles $F(\eta)$, $G(\eta)$, are accelerated as shows in Fig. 4. While opposite trend is recorded in $H(\eta)$ profile as consider in Fig. 4. The influence of (K_2) on $F(\eta)$, $G(\eta)$, and $H(\eta)$ have been demonstrated in Fig. 5. Based on Fig. 5 shows that the depreciating in $F(\eta)$, $G(\eta)$ profiles with mounting value of (K_2). In view of the fact that augmenting (K_2) improves the viscosity of fluid due to this both profiles $F(\eta)$, $G(\eta)$ reduces. Whereas opposite effect has been examined for the profile of $H(\eta)$. Fig. 6 is examined to view that the performance of (Rd) and (Bi) on $\theta(\eta)$. It is noted that $\theta(\eta)$ and their thermal layer thickness augmenting trends of (Rd). In fact, it is proved as the heat is obtained due to radiation process in working fluid so (Rd) increases. And also Fig. 6 explained that the impact of (Bi) on $\theta(\eta)$. $\theta(\eta)$ is the enhancing function of (Bi). Eventually, it is the resistance of internal heat to external heat that is the reason the fluid temperature increases. The influence of (Nt) on $\theta(\eta)$ and $\phi(\eta)$ can be seen in Fig. 7. It is supposed that both profiles are the leading function of (Nt). Thus, growing estimation of (Nt), nanoparticles are accelerated near the colder to hotter surface results enhanced in $\theta(\eta)$ and $\phi(\eta)$. Fig. 8 are plotted to witness the variation in $\phi(\eta)$ for various value of (Ch) and (E). Dilapidated in (Ch) causes to $\phi(\eta)$ profile displayed a tendency to reduce. Actually, destructive rate of chemical reaction uplifts for greater value of (Ch). This has used to dissolve terminate the fluid more proficiently. Fig. 8 elucidated the escalating behavior of (E) on $\phi(\eta)$. In fact, endorses the chemical reaction which ultimately $\phi(\eta)$ rises.

Impact of (K_1) on Nusselt number via Magnetic parameter is sketched in figure-9. Here $Re_r^{-1} Nu$ declines with higher values of (Ma) while reverse trend is seen via. (K_1). The variations of $Re_r^{-1} Nu$ on various physical quantities (Rd), (Nt), (Ch) and (E) are discussed in figures 10-11. Higher values of (Rd) and (E) show $Re_r^{-1} Nu$ is an increasing trend while it is decreases with higher values of (Nt), (Ch).

4. Concluding remarks

The current exploration emphases on Eyring-Powell nanoparticles past a rotating disk via thermal radiation and activation energy has been numerically examined. The influence of various leading parameters is scrutinized through graphic form. Some of the significant features have been given as

- $F(\eta)$, $G(\eta)$ Profiles have increased and decreased behavior with rising of s , K_1 , K_2 and Ma .

- Temperature field $\theta(\eta)$ has amplified due to rising value of Rd , Nt and Bi .
- The concentration distribution has been increased with rising value of E and reduced with rising value of Ch .
- Heat transfer rate is higher with higher values of E while, reverse behavior is noticed with Ch .

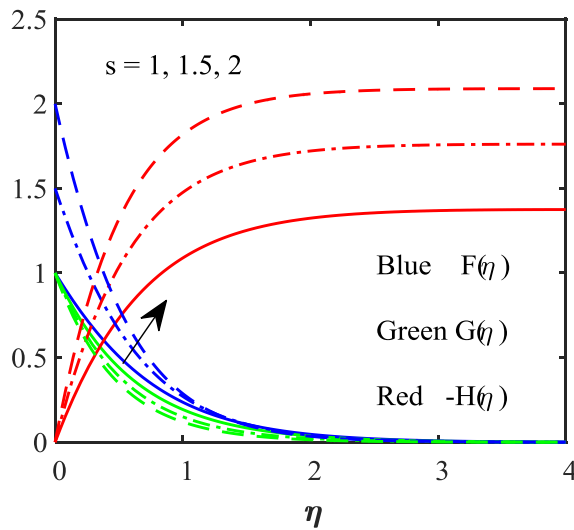


Figure-1. variations of $F, G, -H$ via s

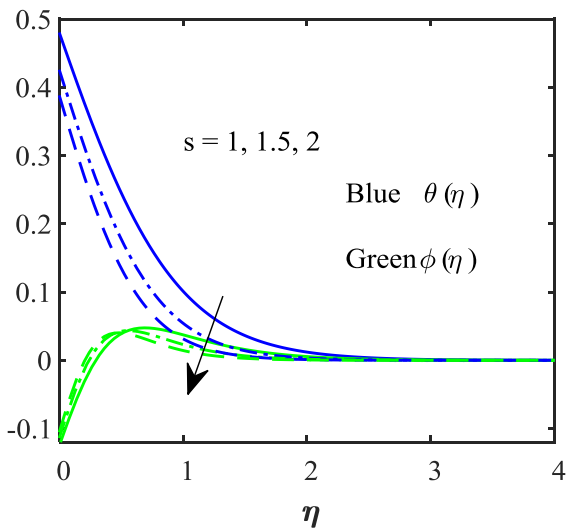


Figure-2. Variations of θ, ϕ via s

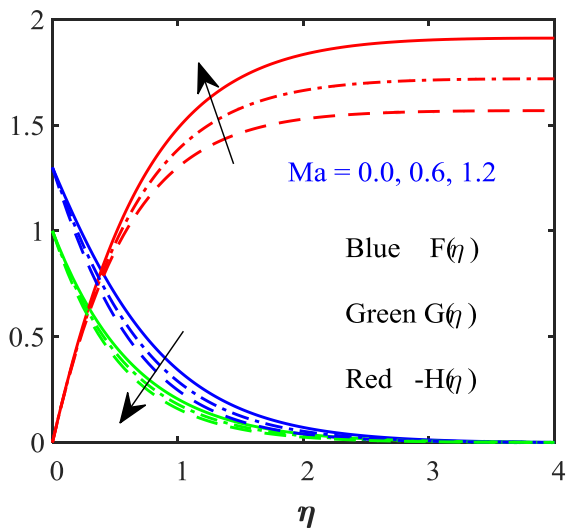


Figure-3. Variations of $F, G, -H$ via Ma

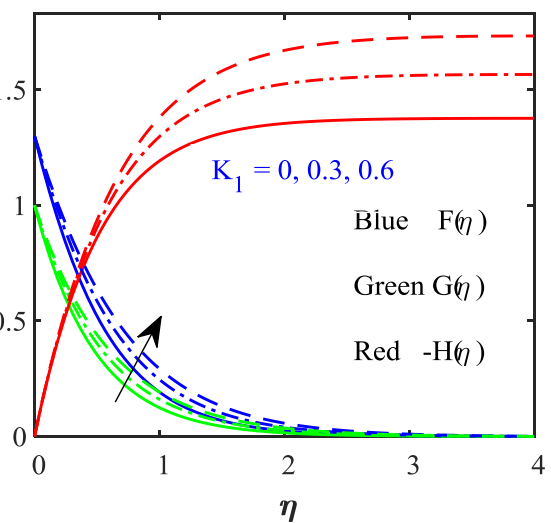


Figure-4. Variations of $F, G, -H$ via K_1

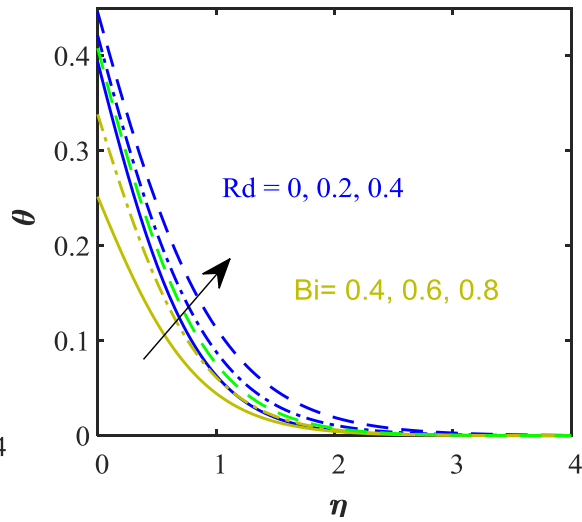
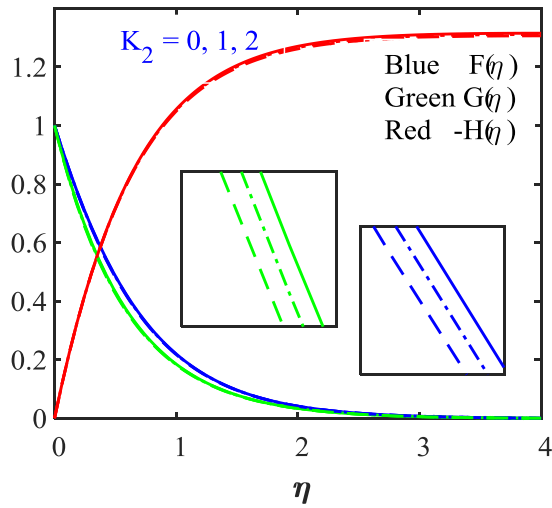


Figure-5. Variations of $F, G, -H$ via K_2 Figure-6. Variations of θ via Rd and Bi

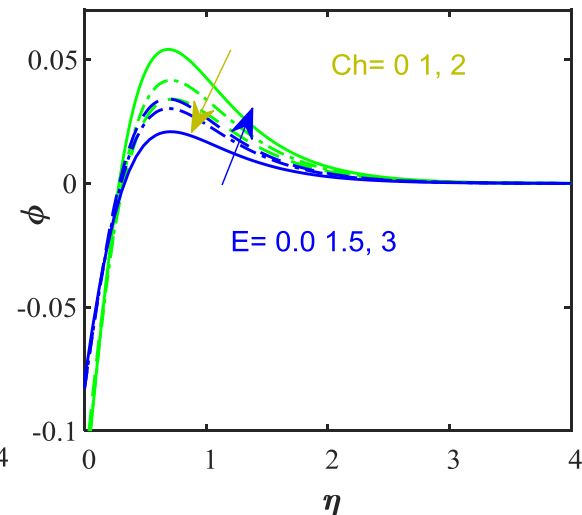
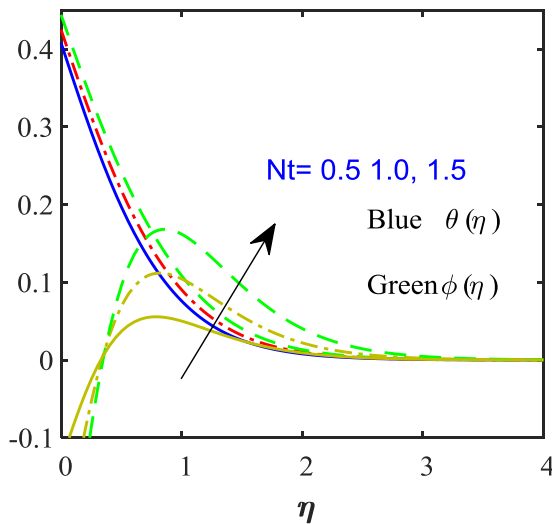


Figure-7. Variations of θ, ϕ via Nt

Figure-8. Variations of ϕ via E, Ch

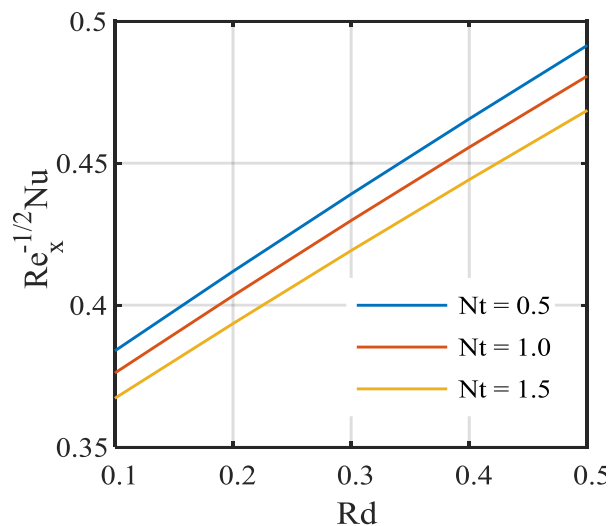
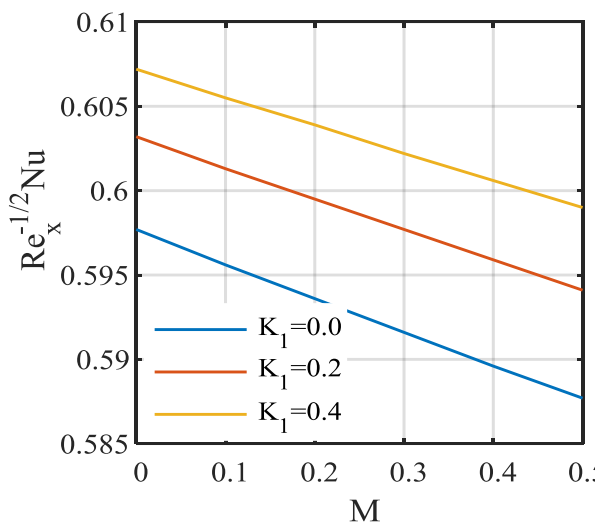


Figure-9. Variations of $Re_x^{-1/2} Nu$ via

Nt, Ma Figure-10. Variations of $Re_r^{-1/2} Nu$ via Rd, Nt

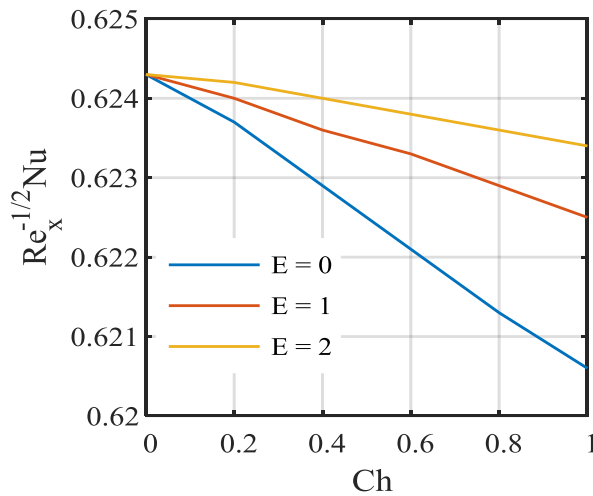


Figure-11. Variations of $Re_r^{-1/2} Nu$ via E , and Ch

Table-1. Comparison table for limiting case of Turkeyilmazoglu[14]

Comparison table for limiting case of Turkeyilmazoglu[14]

M	Previous Results [14]			Present Results		
	$F'(0)$	$-G'(0)$	$-\theta'(0)$	$F'(0)$	$-G'(0)$	$-\theta'(0)$
0	-0.948313	1.486952	0.875662	-0.948565	1.487001	0.875872
2	-1.663452	2.0239449	0.742212	-1.663448	2.023943	0.742545

References

[1] Abbas Z, Sheikh M, Motsa SS, Numerical solution of binary chemical reaction on stagnation point flow of Casson fluid over a stretching/shrinking sheet with thermal radiation, Energy, 2016;95:12–20.

[2] Bachok N, Ishak A, Pop I, Flow and heat transfer over a rotating porous disk in a nanofluid Phys. B: Condens. Matter, 406; 2011:1767-1772.

[3] EL-Dabe NT, Attia HA, Essawy MA. Non-linear heat and mass transfer in a thermal radiated MHD flow of a power-law nanofluid over a rotating disk. SN Appl. Sci. 2019;1: 551 <https://doi.org/10.1007/s42452-019-0557-6>.

[4] Gholinia M, Hosseinzadeh Kh, Mehrzadi H., Ganji DD, Ranjbar AA. Investigation of MHD Eyring–Powell fluid flow over a rotating disk under effect of homogeneous–heterogeneous reactions. Case St. Therm. Eng. 2019; 13:100356.

[5] Hatami M, Sheikholeslami M, Ganji DD. Laminar flow and heat transfer of nanofluid between contracting and rotating disks by least square method. Powder Technol. 2014; 253:769-779.

[6] Hayat T, Makhdoom S, Awais M, Saleem S, Rashidi MM. Axisymmetric Powell-Eyring fluid flow with convective boundary condition: optimal analysis, App. Math. Mech. 37 (2016) 919–928. doi: 10.1007/s10483-016-2093-9.

[7] Ibrahim. W. Three-dimensional rotating flow of Powell-Eyring nanofluid with non-Fourier’s heat flux and non-Fick’s mass flux theory. Res. Phys. 2018; 8:569-577.

[8] J. Buongiorno, Convective transport in nanofluids, ASME J. Heat Transfer 128;

- [9] Jyothi K, Reddy PS, Reddy MS. Influence of magnetic field and thermal radiation on convective flow of SWCNTs-water and MWCNTs-water nanofluid between rotating stretchable disks with convective boundary conditions Powder Technol. 2018;331 : 326-337.
- [10] Khan A, Mustafa M, Hayat T, Farooq MA, Alsaedi A, Liao SJ. On model for three-dimensional flow of nanofluid: an application to solar energy, J. Mol. Liq. 2014; 194:41-47.
- [11] Khan NA, Sohail A, Sultan. F. EFFECT OF ANISOTROPIC SLIP AND MAGNETIC FIELD ON THE FLOW AND HEAT TRANSFER OF EYRING-POWELL FLUID OVER AN INFINITE ROTATING DISK. Int. J. Fluid Mech. Research, 2017;44:257–273.
- [12] Mansur S, Ishak A. Three-dimensional flow and heat transfer of a nanofluid past a permeable stretching sheet with a convective boundary condition. AIP Conf. Proc. 2014; 906:1614.
- [13] Mustafa M. MHD nanofluid flow over a rotating disk with partial slip effects: Buongiorno model. Int. J Heat Mass Trans. 2017; 108:1910-1916.
- [14] Mustafa Turkyilmazoglu. MHD fluid flow and heat transfer due to a stretching rotating disk. Int. J. Therm. Sci. 2012; 51:195-201.
- [15] Pourmehran O. Sarafraz MM, Rahimi-Gorji M, Ganji DD. Rheological behavior of various metal-based nano-fluids between rotating discs: a new insight. J. Taiwan Inst. Chem. Eng. 2018;88:37-48.
- [16] Powell RE, Eyring H. Mechanism for relaxation theory of viscosity, Nature, 154;1944: 427–428.
- [17] Qayyum S, Khan MI, Hayat T, Alsaedi A. Comparative investigation of five nanoparticles in flow of viscous fluid with Joule heating and slip due to rotating disk. Phys. B Condens. Matter, 2018; 534:173-183.
- [18] Qayyum S, Khan MI, Hayat T, Alsaedi A. Tamoor M. Entropy generation in dissipative flow of Williamson fluid between two rotating disks Int. J. Heat. Mass Transf. 2018; 127:933-942.
- [19] Ramzan M, Farooq M., Hayat T, Chung J. D. Radiative and Joule heating effects in the MHD flow of a micropolar fluid with partial slip and convective boundary condition, J. Mol. Liq. 2016;221: 394–400.
- [20] Ramzan M, Chung Jae D, Ullah N, Partial slip effect in the flow of MHD micropolar nanofluid flow due to a rotating disk – A numerical approach, Res. Phys. 7; 2017: 3557-3566.
- [21] Rashidi MM, Abelman S, Freidooni MN. Entropy generation in steady MHD flow due to a rotating porous disk in a nanofluid Int. J. Heat. Mass Transf., 62; 2013:515-525.
- [22] S.U.S. Choi, J.A. Eastman, Enhancing thermal conductivity of fluids with conductivity of fluids with nanoparticles ASME publication- feed, 1995; 231: 729–737.
- [23] Turkyilmazoglu M. Nanofluid flow and heat transfer due to a rotating disk. Com. Fluids 2014; 94:139-146.
- [24] Waqas M, Jabeen S, Hayat T, Khan MI, Alsaedi A. Modeling and analysis for magnetic dipole impact in nonlinear thermally radiating Carreau nanofluid flow subject to heat generation. J. Magn. Mater, 2019; 485: 197-204.
- [25] C. Srinivas Reddy, Kishan Naikoti, MHD Boundary Layer Flow of Casson Nanofluid Over a Non-Linear Stretching Sheet with Viscous Dissipation and Convective Condition, Journal of Nanofluids Vol. 5, pp. 870–879, 2016.

- [26] N.Kishan, Srinivas Maripala and C. Srinivas Reddy, MHD effects on free convective heat and mass transfer in a doubly stratified non-Darcy porous medium, *International Journal of Engineering Science and Technology (IJEST)*, Vol. 3 No.12, 2011.
- [27] C. Srinivas Reddy, N. Kishan, and B. Chandra Shekar, MHD Boundary Layer Flow and Heat Transfer of a Nanofluid Over a Shrinking Sheet with Mass Suction and Chemical Reaction, *J. Nanofluids* 2015, Vol. 4, No. 4